Interplay between nanometer-scale strain variations and externally applied strain in graphene

G. J. Verbiest[1], S. E. Huber[2], M. Andersen[2], C. Stampfer[1], and K. Reuter[2]

[1]RWTH Aachen University, Otto-Blumenthal-Straße 26, 52074 Aachen, Germany
[2]Technische Universität München, Lichtenbergstr. 4, 85747 Garching, Germany
Verbiest@physik.rwth-aachen.de

Abstract

As the thickness of graphene membranes is only one atomic layer, their material properties are highly susceptible to mechanical deformations. In particular, such deformations or strains can be used to tailor the electronic properties of graphene. The effect of strain on the carriers in graphene is generally twofold. First, the area of the unit cell is altered resulting in a redistribution of the charge carrier density in a way that strain variations give rise to effective electron-hole puddles at low carrier densities.[1,2] Second, strain generates a so-called pseudovector potential that is similar to the vector potential of a real magnetic field.[1-6] It is exactly such a strain-induced randomly varying pseudovector potential, which recently has been identified as the limiting mechanism for the carrier mobility in high-quality graphene devices on a substrate.[7-9] As Couto and co-workers[7] showed, these strain variations are on a length scale of a few nanometers such that they act as long-range scattering centers allowing for pseudospin flips. Thus nanometer-scale strain variations enable direct backscattering that limits the carrier mobility in high-quality graphene samples. In fact, it has been shown that the mobility is inversely proportional to the strength of nanometer-scale strain variations.[7] As these strain variations can be non-invasively monitored by the line-width of the graphene specific Raman 2D-line[9], fabrication processes have been recently optimized to suppress strain variations leading to significant improvements in carrier mobility.[10,11] For future optimization a thorough understanding of the interplay between strain variations and external mechanical influences, such as `global' strain are of great importance. Also in view of the promise to tailor electronic properties by strain engineering a detailed knowledge of this particular interplay is crucial.

In this work we present a molecular modeling study analyzing the interplay between strain variations and external mechanical influences in graphene (Fig. 1). Under compressive strain nanometer-scale strain variations may be intricately mingled with the formation of static ripples.[12,13] We therefore focus our analysis on applied tensile strain. As for the physical origin of the nanometer-scale strain variations in graphene, thermal fluctuations as well as frozen ripples from the fabrication process and atomic defects in substrates like hBN are conceivable[12,14], we consider both the effect of thermal fluctuations and of a static Gaussian potential to model defects in a hBN substrate. For both potential sources of nanometer-scale strain variations we observe an intriguing non-monotonic variation of the average atomic displacements with increasing externally applied tensile strain (Fig 2 and 3). Arising from the non-linear elastic properties of graphene, this variation allows us to predict experimentally observable signatures of nanometer-scale strain variations in the measurement of the carrier mobility as well as in the measurement of the line-widths of the Raman active G- and 2D-mode.

The presented insights may be also highly relevant for other two-dimensional crystals with non-linear Young's modulus. As these materials have a unique electromechanical coupling analogous to graphene, a detailed understanding of this interplay is crucial for future applications of these two-dimensional crystals as well.

References

[1] H. Suzuura and T. Ando, Phys. Rev. B, **65** (2002) 235412.
[2] J.L. Manes, Phys. Rev. B, **76** (2007) 045430.
[3] F. de Juan, J.L. Manes, M.A.H. Vozmediano, Solid State Commun., **76** (2013) 175.
[4] N. Abedpour, R. Asgari, and F. Guinea, Phys. Rev. B, **84** (2011) 115437.
[5] K-J. Kim, Ya.M. Blanter, and K-H. Ahn, Phys. Rev. B, **84** (2011) 081401(R).
[6] R. Burgos, J. Warnes, L.R.F. Lima, and C. Lewenkopf, Phys. Rev. B, **91** (2015) 115403.
[7] N.J.G. Couto, D. Constanzo, S. Engels, D.-K. Ki, K. Watanabe, T. Taniguchi, C. Stampfer, F. Guinea, and A.F. Morpurgo, Phys. Rev. X, **4** (2014) 041019.
[8] S. Engels, B. Terres, A. Epping, T. Khodkov, K. Watanabe, T. Taniguchi, B. Beschoten, and C. Stampfer, Phys. Rev. Lett., **113** (2014) 126801.
[9] C. Neumann, S. Reichardt, M. Drögeler, K. Watanabe, T. Taniguchi, B. Beschoten, S.V. Rotkin, and C. Stampfer, Nano Lett., **15** (2015) 1547.
[10] L. Banszerus, M. Schmitz, S. Engels, J. Dauber, M. Oellers, F. Haupt, K. Watanabe, T. Taniguchi, B. Beschoten, and C. Stampfer, Sci. Adv., **1** (2015) 6.

[11] L. Banszerus, M. Schmitz, S. Engels, M. Goldsche, K. Watanabe, T. Taniguchi, B. Beschoten, and C. Stampfer, http://arxiv.org/abs/1511.08601
[12] E.V. Castro, H. Ochoa, M.I. Katsnelson, R.V. Gorbachev, D.C. Elias, K.S. Novoselov, A.K. Geim, and F. Guinea, Phys. Rev. Lett., **105** (2010) 266601.
[13] J.C. Meyer, A.K. Geim, M.I. Katsnelson, K.S. Novoselov, T.J. Booth, and S. Roth, Nature, **446** (2007) 60.
[14] S. Park, C. Park, and G. Kim, J. Chem. Phys., **140** (2014) 134706.

Figures

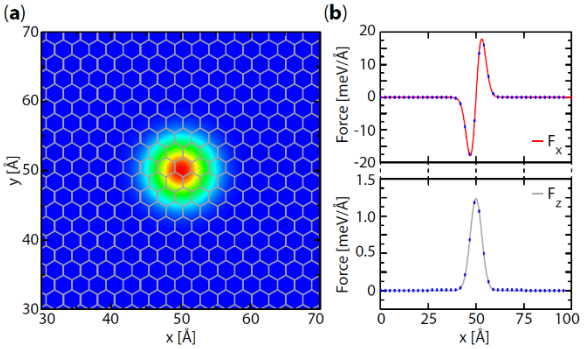

FIG. 1: Illustration of the simulation cell and the applied Gaussian potential. The Gaussian potential has a width of three interatomic carbon-carbon bonds and a strength of +90 meV. (a) Top view of the central area of the graphene sheet with all individual C atoms overlayed with a color map of the Gaussian potential that is applied in the center of the sheet. (b) Force induced by the Gaussian potential on the C atoms of an ideal sheet and along a line at y = 50 Å (red = in-plane force, gray = out-of-plane force, lines are superimposed to guide the eye).

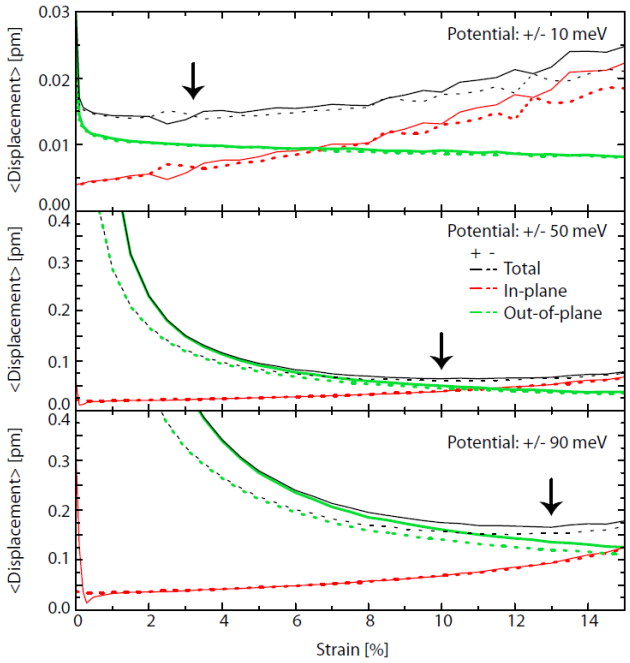

FIG. 2: Calculated average displacements under the influence of a static Gaussian potential. Shown as a function of applied equibiaxial tensile strain are the total displacement (black curves), the in-plane displacement (red curves), and the out-of-plane displacement (green curves). The upper panel corresponds to a strength of the Gaussian potential of 10 meV, the middle panel to 50 meV, and the lower panel to 90 meV. In all panels, solid curves correspond to a repulsive potential and dotted curves to an attractive potential. The arrows indicate the minimum in total displacement.

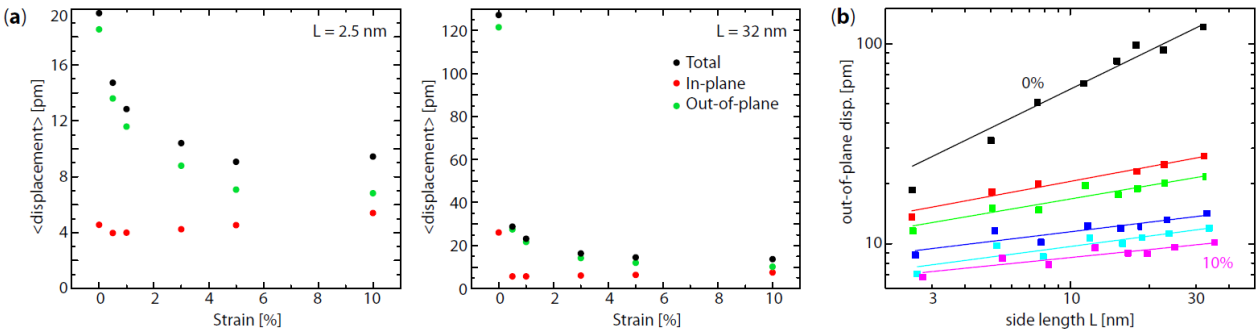

FIG. 3: Calculated time-average displacements as a function of strain from MD simulations at 300 K. (a) Results are shown for a side length L of 2.5 nm (left panel) and 32 nm (middle panel). In agreement with the MM simulations, the out-of-plane displacement decreases with increasing strain, whereas the in-plane displacement increases. (b) The average out-of-plane displacement scales with the side length L for different values of strain: 0% (black), 0.5% (red), 1% (green), 3% (blue), 5% (cyan), 10% (magenta). The slope of the fitted lines yields the critical exponent of membrane theory.